ISAL 2025
16. International Symposium on Automotive Lighting
Darmstadt, 22. – 24. September 2025
Article DOI: 10.26083/tuprints-00030888
DOI (proceedings): 10.26083/tuprints-00030825

# Comparison of Different Adaptive Light Distributions for Automated Driving

N. Müller[1], M. Waldner[1], T. Bertram[1]

1: TU Dortmund University, Institute of Control Theory and Systems Engineering (RST), Dortmund, Germany

## 1. Abstract

The contribution at hand compares nine innovative adaptive luminous intensity distributions (LIDs) for automated driving, as human-focused LIDs are mostly inefficient for computer vision. The adaptive LIDs are categorized into object-based and material-based LIDs. The advantages and disadvantages, as well as the requirements for the functionality of each LID, are discussed. All adaptive LIDs plus two reference LIDs are evaluated for camera object detection with neural networks in a worst-case scenario. Additionally, the robustness against object position or localization errors is tested. The results show that material-based LIDs outperform all others, e.g., by an improvement in detection confidence of 24% compared to one variant of object-based lighting. When considering inaccuracies, the object-based LIDs yield poor results. In contrast, those that only require a static 3D environment model show an improvement of 186% in terms of confidence and 178% in terms of Intersection over Union (IoU) compared to the best-scoring object-based LID.

*Keywords: matrix headlight, computer vision, automated driving, optimization*

## 2. Introduction

Automated driving vehicles rely on sensors, such as cameras, for safe interaction with their environment. However, today's headlamp LIDs are optimized for human vision and are inefficient in terms of safety and energy for camera-based computer vision [1], especially in challenging light conditions. Thus, new adaptive LIDs are necessary to support the neural network-based detection of traffic objects, ensuring the safety of automated driving vehicles and preventing accidents. Previous research [1, 2] has shown that one possibility to enhance computer vision and simultaneously save energy is a material-based LID. The material-based LID illuminates each material in the environment with an individual luminous intensity $I_\mathrm{v} \in \mathbb{R}_{\geq 0}$, utilizing the materials' distinct colors and reflective properties to enhance computer vision. The difference in camera object detection between the human-focused realistic high beam (HB) and the optimal material-based LID is illustrated in the simulation in Fig. 1. With HB only a neural network confidence of 0.36 can be achieved. In contrast, with the material-based approach the confidence is 0.81. Another approach to improve object detection is to selectively illuminate detected objects and their surroundings based on the estimated class and the bounding box (BBox) [3]. Both approaches also have different variations. For example, it can make a difference whether the BBox of an object-based LID is illuminated homogeneously or with a Gaussian-shaped LID inside of the BBox [4].


(a) Illumination with a HB LID. (b) Optimal material-based illumination.

Figure 1: Confidence and BBoxes of a neural network-based detection for a pedestrian with different LIDs in the simulation [1].

The contribution at hand presents and discusses the advantages and disadvantages of nine different LIDs designed for computer vision, focusing on material-based and object-based LIDs. This also includes the requirements for the LIDs' functionality. Each LID, in addition to realistic low beam (LB) and HB for reference, is evaluated regarding the neural network-based detection quality and its robustness against inaccurate object detection and localization errors. The results show that the material-based LIDs with prior object information outperform all other LIDs. For example, the most detailed material-based LID performs 24% better in terms of confidence and 19% better in terms of IoU, $IoU \in \mathbb{R}_{\geq 0,\leq 1}$, compared to an object-based LID with a homogeneously illuminated BBox. However, when considering the inaccuracies, only HB and the material-based LIDs without object information can achieve object detection with a confidence level of over 0.54. In contrast, the confidence of all other LIDs, including the object-based LIDs, is at most 0.21.

# 3. Adaptive Light Distributions for Automated Driving

The contribution at hand focuses on two main approaches for adaptive LIDs that can support object detection in automated driving. The first approach involves object-based lighting, where the detected objects are selectively illuminated with a special LID that is based on their estimated class and position. The rest of the environment is illuminated differently, e.g., to create a greater contrast of the objects to the back-ground. In this contribution, different variants of object-based LIDs are discussed.

The first analyzed object-based LID #ocp creates an object-contour-precise homogenous illumination of the object different from the rest. To achieve this, the object must be detected first with its correct class in the camera image of the automated driving vehicle. For precise illumination, the exact contour of the object must be known, e.g., through a segmentation neural network. An example of #ocp is shown in Fig. 2a. The second object-based LID #obh creates an illumination such that the BBox of the object, which is a rectangle in the camera image, is illuminated homogeneously and differently from the environment. This LID also requires object detection with the object class first, but this time, only the BBox in the camera image needs to be known and no segmentation is needed. Thus, it requires less specific information than #ocp. The LID #obg is similar to #obh, with the difference that it has no homogeneous LID inside the object's BBox but a Gaussian-shaped LID [4]. This leads to the middle of the BBox being illuminated brighter than its edges. Example for #obh and #obg are shown in Fig. 2b and Fig. 2c. A Gaussian distribution with a standard deviation of the maximum BBox dimension, e.g., the height of a pedestrian's BBox, is multiplied by the $I_v$ target value in the center to create #obg.

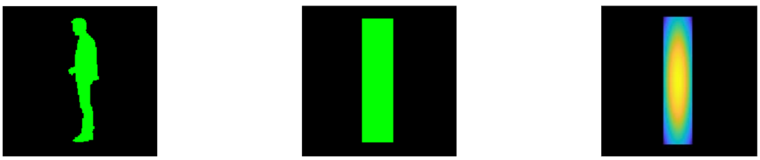

(a) Object-precise, #ocp. (b) BBox-precise, #obh. (c) BBox Gaussian, #obg.

Figure 2: Schematic illustration of the three object-based LIDs.

The second discussed approach as a suitable LID for computer vision is material-based lighting. This type of LID determines different $I_v$ levels for different surface materials, such that each material in the environment can be illuminated differently bright. The approach considers that materials or surfaces have different reflective behaviors or colors, which impacts the reflection of light and the material's appearance. The $I_v$ of each material in the environment can be adjusted such that neural network-based detection in camera images is improved while simultaneously saving energy [1, 2]. All material-based LIDs in this contribution require a 3D environment model, including the vehicle's localization within it. However, depending on the type of material-based LID, no further information is necessary beyond that.

The material-based LID #m19o distinguishes between 19 different materials plus one default material for unknown materials. Thus, 20 different $I_v$ can be used to selectively illuminate the environment. An overview of the material division for an example scene is shown in Fig. 3. As visible, there is also a material for stationary or dynamic detected objects like pedestrians or vehicles, allowing them to be contour-precisely illuminated, like with #ocp. However, this also means that prior knowledge of the object, like with #ocp, #obh and #obg, is required. In contrast to all previously mentioned LIDs, LID #m19 illuminates the environment selectively based on only the surface materials of static objects, e.g., traffic lights, but without any knowledge of dynamic detected objects, resulting in 19 different $I_v$. This means #m19 requires only a static 3D environment model with material coding, without an object material or similar for the dynamic or stationary objects. The main advantage is that #m19 is independent of these objects. Thus, also no dynamic object position information, image segmentation or object classification is necessary. The stationary or dynamic objects are illuminated with an $I_v$ of the materials behind them. The material segmentation for #m19 is similar to Fig. 3 for #m19o, except for no object material.

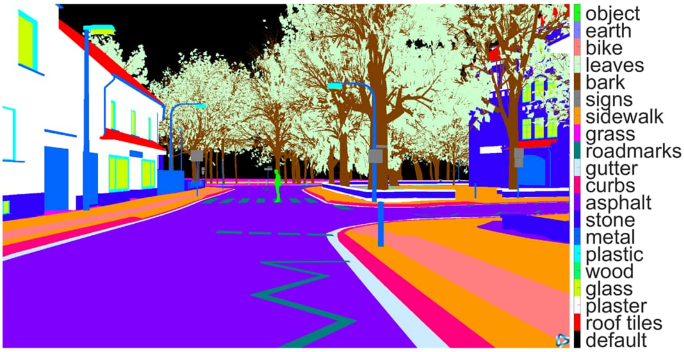


Figure 3: Material-coded environment for the material-based LID #m19o. Each material can be illuminated with a different $I_v$.

There are four more material-based LIDs considered in this contribution. The LIDs #m10o, #m10, #m3o, and #m3 work similarly to #m19o and #m19 respectively, but with the difference that the material segmentation of the environment is adapted and materials are grouped. For #m10o, the environment has 10 distinguished materials, including one default material and an additional object material. The material amount is reduced and #m10o includes only those from the previous 19 from #m19o that illuminate traffic-relevant surfaces or highly reflective surfaces, i.e., asphalt, gutters, curbs, sidewalks, bike paths, and road markings. The remaining materials are combined to a new default group. The new material segmentation for #m10o is shown in Fig. 4a. Similar to #m19, #m10 includes no object material or dynamic object knowledge and, thus, only 9 different materials plus one default one. #m3o and #m3 reduce the amount of material distinguishment even more into simple material classes. This results in one diffuse material, consisting of diffuse traffic-related materials, one reflective material, one default material and for #m3o, one object material. The diffuse material includes the previously distinguished materials asphalt, gutters, curbs, bike paths, and sidewalks. The reflective material includes previous glass, metal, signs, and road marking materials. The material coding for the LID #m3o is shown in Fig. 4b. For #m3, it is similar but without the object material. The advantage of fewer materials in the environment lies in being more robust due to potential spatial inaccuracies of the illumination, less detailed information for the material coding being needed and the faster determination of an optimal $I_v$ for each material. However, the illumination is not as selective as with more materials.

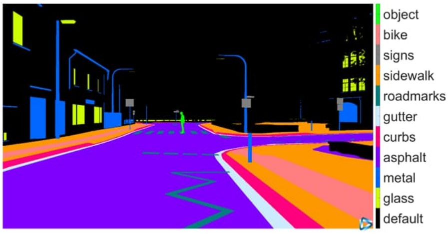


(a) Materials for LID #m10o.

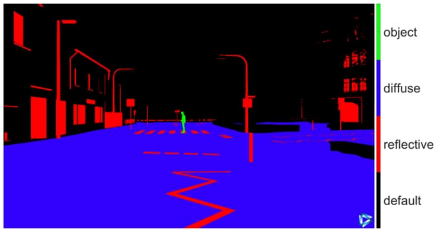


(b) Materials for LID #m3o.

Figure 4: Material-coded environment for the material-based LIDs #m10o and #m3o, respectively. Each material can be illuminated with a different $I_v$.

An overview of the requirements for each LID is presented in Tab. 1. The main disadvantage of all object-based LIDs (#ocp, #obh and #obg) is that the first detection of the object is necessary before the object-based illumination is even possible. Thus, these LIDs are attractive when an object has already been detected once, improving the existing detection. The same applies to the material-based LIDs #m19o, #m10o and #m3o, which require prior object knowledge for precise illumination. However, even if there is an object detection, it could also be a false positive detection or a true positive detection with incorrect BBoxes or a misfitting object contour. When illuminated with an unfitting illumination due to poor detection beforehand, the detection performance can even worsen. So, LIDs that require prior knowledge of the objects are very sensitive to the object detection performance before they are even applied. In contrast, #m19, #m10, and #m3 do not require any information about the existence or position of an object, which is also the main advantage of these LIDs.

Table 1: Requirements for the functionality of the adaptive LIDs.

| | Prior object detection | BBox in Camera image | Object segmentation | 3D environment model |
|---|---|---|---|---|
| #ocp | × | | × | |
| #obh | × | × | | |
| #obg | × | × | | |
| #m19o | × | | × | × |
| #m19 | | | | × |
| #m10o | × | | × | × |
| #m10 | | | | × |
| #m3o | × | | × | × |
| #m3 | | | | × |

While #ocp, #m19o, #m10o, and #m3o require contour-precise information for illumination, which can be acquired, e.g., through image segmentation neural networks, #obh and #obg only need the object's BBox in the camera image. This makes the latter two LIDs more robust to detection errors, as the more precise information is required, the more prone it is to errors. Also, the contour-precise illumination is very sensitive to small details of the object, or, for example, if the object is a pedestrian, to the pose of the person, especially that of the limbs.

The primary disadvantage of all material-based LIDs is that they require a 3D environment model. If a 3D environment model is available, it can be distinguished into different materials with minimal effort using automated algorithms. Since increasingly 3D environment models are available for automated driving purposes or, e.g., virtual city tours, it is conceivable that the required information for material-based LIDs will become more widespread in the future. Nevertheless, material-based LIDs are susceptible to model errors in the environment or when the environment changes after the model is created. However, for automated driving, the errors of environment models, such as high-definition maps, must be beneath 0.01 m [5, 6]. Thus, in this contribution, it can be assumed that when automated driving vehicles require this anyway, the impact of model error can be neglected. Generally, it is more feasible to have a static 3D environment model than to have prior object information in real-world road traffic, which makes #m19, #m10, and #m3 more realistic for a real nighttime drive. However, once the object is detected, #obh and #obg seem appealing because they are independent of other information sources. Therefore, a combination might be optimal, but this is not discussed in this contribution.

# 4. Experiment and Results

The experiments are conducted in the verified headlight simulation developed by TU Dortmund University [1, 7] using Unreal Engine 5.2 with a precise 3D environment model of the German city of Lippstadt created by 3D Mapping Solutions GmbH. The task of the ego vehicle is to detect a black-dressed pedestrian that is positioned 25 m in front of the ego vehicle at the center of the driving lane. There is no external street lighting to resemble a worst-case scenario. The scene is the same as shown in Fig. 3 and Fig. 4, with the same material segmentations. For object detection, the neural network YOLOv8 [8] is used without additional training for the specific scenario. Thus, the aim is to achieve similar good detection as in the daytime, with the major advantage of avoiding time-consuming neural network training or the difficulties of acquiring large datasets. A pair of matrix headlights, each with $640 \times 160$ pixels, a horizontal opening angle of 40°, and a vertical opening angle of 10°, creates the illumination of the environment with the LIDs. Therefore, each headlight has the same 4:1 aspect ratio as the real Porsche headlights [9], and their real LB and HB LIDs can be used for reference with a cubic upscaling. Other than that, all nine LIDs presented in Sec. 3 are investigated.

The objective metric of the detection quality costs $c_{\mathrm{q}}(\boldsymbol{D}) \in \mathbb{R}_{\geq 0, \leq 1}$ from [10] is applied to optimize the performance of different adaptive LIDs in neural network object detection. For this, an adapted optimization loop of [2], as shown in Fig. 5, is used, where the $I_{\mathrm{v}}$ per material for #m19o to #m3, or the $I_{\mathrm{v}}$ for objects and the $I_{\mathrm{v}}$ for the rest of the environment for #ocp to #obg is optimized to minimize $c_{\mathrm{q}}(\boldsymbol{D})$.

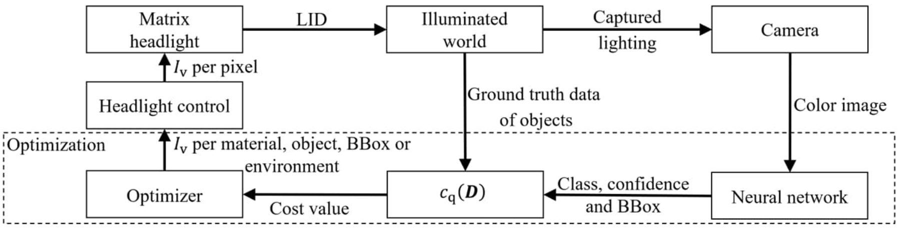


Figure 5: Optimization loop for the $I_v$ of the LIDs [2].

$c_q(\boldsymbol{D})$ depends on the detections $\boldsymbol{D} \in \mathbb{R}^{n_D \times 1}$ with $n_D$ detected objects by YOLOv8 [10]. It includes the detection rate, which uses the number of true positive detections $TP$, false positive detections $FP$ and false negative detections $FN$. In addition, $c_q(\boldsymbol{D})$ consists of the confidence $C \in \mathbb{R}_{\geq 0, \leq 1}$ in $TP$, and the $IoU$ of $TP$, which measures the fit of the BBoxes compared to the ground truth. $c_q(\boldsymbol{D})$ is a weighted addition of these components as

$$c_q(\boldsymbol{D}) = 0.5\left(1 - \left(\frac{TP}{(FP + FN + TP)}\right)\right) + \\ +0.25\left(1 - \left(\frac{\sum IoU}{(FN + TP)}\right)\right) + 0.25\left(1 - \left(\frac{\sum C}{(FN + TP)}\right)\right). \quad (1)$$

The optimization results for all nine adaptive LIDs and the reference LIDs LB and HB are shown in Tab. 2. In addition to the cost value of $c_q(\boldsymbol{D})$, which should best be minimal, $C$ in the pedestrian detection and the $IoU$ of it are presented, which should best be maximal. For creating the illumination, all results in Tab. 2 assume a perfectly detected object contour for #ocp, #m19o, #m10o and #m3o, perfectly detected BBoxes for #obh and #obg, and a perfectly located ego vehicle for #m19o, #m19, #m10o, #m10, #m3o and #m3.

Table 2: Evaluated object detection metrics for all LIDs with illumination perfectly matched to the environment and objects. The best values are shown in bold.

| | #ocp | #obp | #obg | #m19o | #m19 | #m10o | #m10 | #m3o | #m3 | LB | HB |
|---|---|---|---|---|---|---|---|---|---|---|---|
| $c_q$ | 0.08 | 0.12 | 0.10 | **0.05** | 0.09 | **0.05** | 0.11 | **0.05** | 0.12 | 1.00 | 0.13 |
| $C$ | 0.76 | 0.67 | 0.72 | **0.83** | 0.77 | **0.83** | 0.77 | 0.82 | 0.72 | 0.00 | 0.74 |
| $IoU$ | 0.94 | 0.83 | 0.86 | **0.99** | 0.85 | 0.98 | 0.80 | 0.97 | 0.78 | 0.00 | 0.76 |

The results show that the material-based LIDs with additional prior object knowledge, #m19o, #m10o and #m3o, outperform all other LIDs regarding $C$ and $IoU$. $C$ is 0.82 or 0.83, and $IoU$ is almost perfect with 0.97 to 0.99. Concerning the material segmentation, there are only minimal differences in those values, so for this type of LID, it is not that important that there are many different materials. However, if there is no prior information about the object as for #m19, #m10 and #m3, the differences between the number of segmented materials are up to 0.05 for $C$ or 0.07 for $IoU$. Thus, the finer material differentiation shows a small impact on these LIDs. All three LIDs have a decent object detection performance even without object information, e.g., #m19, with a $C$ of 0.77 and an $IoU$ of 0.85.

Compared to the material-based illuminations without object knowledge, only #ocp performs similarly with a $C$ of 0.76 and an $IoU$ of 0.94. The others, #obh and #obg, have similar $IoU$ values as #m19, but with a worse $C$. For example, #obh has a worse $C$ by 0.10. The similar or better $IoU$ is caused by the selective object contour or BBox illumination, which #m19, #m10 and #m3 are not capable of. Thus, it is unexpected that they can compensate by material-based illumination, #m19 and #m10 even achieving a better $C$ than #obh and #obg. In general, #obh is the worst LID of the adaptive nine regarding $C$. This finding is consistent with other research [4], which shows that the BBox illumination performs worse than a Gaussian-shaped one. However, its $IoU$ is by 0.07 better than the $IoU$ of HB. Compared to the adaptive LIDs, HB also enables good camera object detection with a $C$ of 0.74 and an $IoU$ of 0.76. Nevertheless, [1] shows that when the pedestrian stands on the sidewalk and is not directly in front of the ego vehicle, HB can fail to detect the pedestrian at all, as it is a center-focused LID. With LB, detection is not possible at all.

The LIDs of Tab. 2 with the same $I_v$ per pixel are also applied to the same scenario but with an assumed position inaccuracy of 0.1 m and an angular inaccuracy of 2°, which are common localization errors [5, 6]. The aim is to investigate how object-based LIDs perform with misfitting contours or BBoxes and how material-based LIDs perform with localization errors. For each LID, 26 measurements are evaluated, where the ego vehicle is placed in a grid of 0.1 m around the original position with angular offsets of -2°, 0°, and 2°, in addition to the original position with offsets of -2° and 2°. Tab. 3 shows the averaged results for $c_q$, $C$ and $IoU$ over all 26 poses.

Table 3: Evaluated object detection metrics for all LIDs with localization and object detection offset, averaged over 26 measurements per LID, best values in bold.

| | #ocp | #obh | #obg | #m19o | #m19 | #m10o | #m10 | #m3o | #m3 | LB | HB |
|---|---|---|---|---|---|---|---|---|---|---|---|
| $c_q$ | 0.78 | 0.73 | 0.73 | 0.77 | 0.24 | 0.73 | 0.20 | 0.74 | 0.19 | 0.88 | **0.14** |
| $C$ | 0.11 | 0.21 | 0.20 | 0.14 | 0.54 | 0.18 | 0.60 | 0.15 | 0.55 | 0.05 | **0.65** |
| $IoU$ | 0.26 | 0.27 | 0.27 | 0.24 | 0.72 | 0.27 | 0.75 | 0.27 | 0.76 | 0.11 | **0.78** |

Generally, all LIDs suffer from inaccuracies, except for LB, whose performance is slightly improved. For HB, $C$ is by 0.09 lower with 0.65, and $IoU$ remains similar with a difference of 0.02 with 0.78, which makes HB the best LID for inaccuracies in this scenario, as the pedestrian stands in the bright centre spot of the HB. The small variations in the position and rotation of the ego vehicle do not significantly change the light emitted onto the person. In this order, #ocp, #m19o, #m3o and #m10o perform worst of the adaptive LIDs. This is because they depend the most on precise object information of all LIDs, and thus, they are more error-prone when the information is unprecise. For example, for #ocp, the precise contour illumination is moved away from the person by small changes in the position and orientation of the ego vehicle. #obh and #obg fare better, e.g., #obh with a by 0.10 improved $C$ of 0.21 compared to #ocp, but still, $C$ and $IoU$ are low compared to a possible maximum of 1. This can be caused by a BBox illumination requiring less precise information and object fitting than when illuminating the pedestrian contour. In contrast, #m19, #m10, and #m3, which rely solely on the static 3D environment model, perform significantly better than the other adaptive LIDs, which depend on prior object information. Here, object variations are only indirectly considered during optimization. For example, #m10 achieves a $C$ of 0.60 and an $IoU$ of 0.75. This represents an improvement of 186% and 178%, respectively, compared to the best LID with dependence on dynamic object knowledge, #obh. The results for #m10 are also not that different from the best-scoring HB. Despite the already worse results than #m19, #m10, #m3 and HB, the object-based LIDs have a small advantage over the material-based LIDs in this evaluation setup. This is because the object contour and BBox used for headlight control still roughly match the ground truth, as they are the same as before for the results in Tab. 2, even if the illumination has an offset. However, the detected contour could also be non-human shaped, or the BBox might not fit the real one.

In general, the results indicate that object detection benefits from the independence of dynamic or stationary object information, particularly when there are inaccuracies. Even if there is a localization error of 2° and 0.1 m, the LIDs that only depend on the static 3D environment model are more reliable and, thus, more robust for object detection and safer for automated driving. In addition, as mentioned in Sec. 3, it is more realistic to have a static 3D environment model in a real vehicle than to have prior object knowledge, as the appearance of dynamic objects cannot be planned. However, the results in Tab. 2 and 3 are only for a single scenario, and thus, they are not generally valid. Also, the results are based on a static scenario without moving objects, assuming prior knowledge of the object and/or environment, which are still ideal conditions, albeit with inaccuracies.

# 5. Conclusion and Outlook

The contribution at hand presents and compares multiple adaptive LIDs optimized for automated driving to enhance the camera object detection performance. The material-based LIDs outperform the object-based LIDs by at least 0.07 regarding confidence and 0.05 regarding $IoU$, if prior object information and a 3D environment model are available. In contrast to object-based LIDs, which always require object information, there are also material-based LIDs that only rely on the static 3D environment model, which is more likely to be known beforehand than randomly appearing objects in a real night drive. However, they are sensitive to changes in the environment, e.g., construction sides. Both categories of adaptive LIDs outperform LB or HB in terms of object detection quality. However, all LIDs, including HB, perform worse when considering inaccuracies. Only HB and the material-based LIDs without object information achieve a confidence between 0.54 and 0.65, while the LIDs that depend on object knowledge perform poorly with at most 0.21 confidence.

Future work includes the further investigation of new adaptive LIDs for automated driving that do not require prior object information or a localized vehicle in a 3D environment model. Then, the LIDs are more robust and better applicable in a real vehicle. Additionally, the presented optimization process cannot be run during nighttime drives or when moving objects are present.

## 6. References

[1] N. Müller, M. Waldner, and T. Bertram, "Matrix Headlights and Surface Properties: A New Way to Boost Computer Vision and Save Energy for Automated Vehicles," International Congress SIA VISION, 2024.

[2] N. Müller, M. Waldner, and T. Bertram, "Improving Computer Vision by Virtual Optimization of Matrix Headlights Using Surface Properties," International Conference ACDSA, 2024.

[3] F. Barmeyer, et al., "System and method for object-based control of a high-resolution headlight for a motor vehicle," DE102015016375A1, 2015.

[4] S. Cladé, G. Planche, K. BEEV, R. Mezari, and M. Mimoun, "High Definition Lighting solutions to complement camera and improve AEB Effectiveness at Night," International Congress SIA VISION, 2024.

[5] T. G. R. Reid, et al., "Localization Requirements for Autonomous Vehicles," SAE International Journal of Connected and Automated Vehicles, vol. 2, 2019.

[6] K. Rehrl, and S. Gröchenig, "Evaluating Localization Accuracy of Automated Driving Systems," Sensors, vol. 21, 2021.

[7] M. Waldner, N. Müller, and T. Bertram, "Hybrid Rapid Prototyping of Lighting Functions for Humans and Machines," ATZ worldwide, vol. 127, 2025.

[8] Ultralytics (Ed.), "YOLOv8," May 2025. [Online]. Available: https://github.com/ultralytics/ultralytics.

[9] Porsche (Ed.), "Performance leap in light technology," Dec. 2022. [Online]. Available: https://newsroom.porsche.com/en/2022/innovation/porsche-led-mainheadlights-with-hd-matrix-beam-light-technology-30770.html.

[10] N. Müller, F. Glatzel, M. Waldner, and T. Bertram, "Virtual Optimization of Matrix Headlights for Improved Automated Object Detection and Energy Efficiency," International Symposium on Automotive Lighting 2023, 2023.